A Noninvasive Quantification Approach for Monitoring Brain Metabolic Alterations After Surgical Intervention in Ischemic Cerebrovascular Disease

Min Wang
Shanghai University
Bixiao Cui
Xuanwu Hospital Capital Medical University
Yi Shan
Xuanwu Hospital Capital Medical University
Hongwei Yang
Xuanwu Hospital Capital Medical University
Zhuangzhi Yan
Shanghai University
Lalith Kumar Shiyam Sundar
Medical University of Vienna: Medizinische Universitat Wien
Ian Alberts
University of Bern: Universitat Bern
Axel Rominger
University of Bern: Universitat Bern
Kuangyu Shi
University of Bern: Universitat Bern
Yan Ma
Xuanwu Hospital Capital Medical University
Jiehui Jiang
Shanghai University
Jie Lu (imaginglu@hotmail.com)
Xuanwu Hospital Department of Radiology https://orcid.org/0000-0003-0425-3921

Research Article

Keywords: ischemic cerebrovascular disease, glucose metabolism, vascular territory, noninvasive quantification, PET/MR

Posted Date: October 18th, 2021

DOI: https://doi.org/10.21203/rs.3.rs-958601/v1

Abstract

Purpose: Non-invasive quantification of cerebral metabolic rate for glucose (CMRGlc) and characterizing cerebral metabolism of cerebrovascular territories are useful for the understanding of ischemic cerebrovascular disease (ICVD). Here, we proposed a non-invasive quantification approach based on image-derived input function (IDIF) suitable for ICVD patients and monitored the pathophysiological changes after surgical intervention.

Methods: Sixteen healthy controls and 26 ischemic cerebrovascular disease patients with baseline and after surgical visits underwent ^{18}F-FDG PET/MR imaging. The voxel-wise CMRGlc maps were derived *via* our proposed IDIF method. The CMRGlc and standardized uptake value ratio (SUVR) maps were subsequently used to extract quantitative values within 7 volumes of interest (gray matter, white matter, anterior, middle, and posterior cerebral artery, basilar artery, and cerebellar artery territory). Intraclass correlation coefficient (ICC) and absolute percentage error were employed to measure consistency in healthy controls. The quantitative differences of healthy controls and patients at baseline and after surgical visits were statistically analyzed.

Results: For healthy controls, there were no significant differences for region CMRGlc values across bilateral and unilateral IDIF measurements (ICC: 0.91-0.98). Significant differences in CMRGlc were observed across the cohorts in all territories (P< 0.001). The CMRGlc values in the ipsilateral side were significantly increased after surgery intervention (P < 0.05) for all territories (percentage changes: 7.4%~22.5%). Only the posterior cerebral artery and basilar artery territories (-2.8% and 1.9%) were significant differences for SUVR (P < 0.05). The diagnostic ability of CMRGlc in various territories (area under curve: 0.923-0.966) was significantly higher than of SUVR. There was a significant association between CMRGlc with the national institutes of health stroke scores (r: -0.54, P = 0.0041).

Conclusion: These observations suggested the non-invasive quantification approach based on IDIF allowed the individual metabolism measurement of cerebrovascular territories after surgery and identified the glucose pathology changes underlying territories.

Introduction

Ischemic cerebrovascular disease is caused by progressive steno-occlusive disease at the terminal portion of the internal carotid artery (ICA) or middle cerebral artery (MCA) which lead to a cascade of metabolic and molecular changes resulting in cerebral vasculature damage and brain function disturbance [1]. For clinical interventions of ischemic cerebrovascular disease, the concepts of pathophysiological changes that lead to irreversible tissue damage and of the advances in cerebral compensate based on brain-feeding arteries should play a critical role. Therefore, the quantification of pathophysiological changes and regional metabolism is important which may be benefitted to monitor the clinical outcome and recovery effect [2-4].

Maintaining normal brain homeostasis is an energy-consuming process that depends on a continuous supply of glucose. [18F]-Fluoro-2-deoxy-D-glucose (^{18}F-FDG) positron emission tomography (PET) with [^{18}F]-Fluoro-2-deoxy-D-glucose (^{18}F-FDG) is a frequently used imaging technique for assessing brain metabolism in animal and human with ischemic cerebrovascular disease. Brain PET quantification in ischemic cerebrovascular disease involves the determination of specific territories glucose retention in the presence of confounds from infraction area (ischemic core) may differ in subjects. The growing application of PET imaging in ischemic cerebrovascular disease study and clinical trials emphasizes the need for accurate quantitative analyses for target-specific cerebral arteries and tissues [3, 5-8]. Kao et al reported that glucose metabolism may be a powerful tool to evaluate the change of successful surgery in patients with chronic severe carotid stenosis or occlusion [9]. Yu et al also demonstrated that cerebral glucose metabolism has been used in cerebrovascular disease to track the glucose consumption in the cerebral territories [3, 10, 11]. Our previous work has investigated the cerebral hemodynamic patterns and metabolism in patients with symptomatic ischemic

cerebrovascular disease [12]. However, few studies have focused on absolute quantitative on ^{18}F-FDG uptake to evaluate patients with ischemic cerebrovascular disease after treatment.

Currently, the quantification calculation of the cerebral metabolic rate of glucose (CMRGlc) based on ^{18}F-FDG PET requires the additional information from the arterial input function (AIF), which is typically measured by invasive serial arterial blood sampling and difficult for widely promotion in clinics [13]. Meanwhile, standardized uptake value ratio (SUVR), the most popular semi-quantification measure index in PET studies, may be inaccurate because of the overlap of the reference region (contralateral cerebellum) and the individual infraction area [14]. Further, such semi-quantification is often very helpful for clinical diagnostic purposes, yet which may not represent measures of tissue function or composition. They are difficult to provide sensitive and complete information about underlying pathophysiological mechanisms, such as the changes of cerebellar artery territory. Taken together, an alternative quantification technique is required for cerebrovascular disease.

With the advancing of fully integrated PET/MR, previous studies have developed various non-invasive quantification methodologies which extract an image-derived input function (IDIF) from dynamic PET images to avoid the need for the arterial blood sampling [5, 15-17]. However, the clinical value of the IDIF method has not been widely validated in cerebrovascular diseases. Especially in previous IDIF implementations, a blood-pool region, usually bilateral ICA, was extracted as target region to generate IDIF. However, IDIF quantification within ischemic cerebrovascular disease maybe suffer from the specific pathophysiological symptom (unilateral steno-occlusive ICA) which caused the failure of bilateral ICA to track metabolic activity. Ischemic cerebrovascular disease quantification based on IDIF methodology had been restricted that the adoption of IDIF required further methodology modification to enable the unilateral ICA to generate effective IDIF.

Therefore, we hypothesized that the IDIF method based on unilateral ICA could be adopted to perform non-invasive quantification and then address the ischemic cerebrovascular disease quantification challenges. In this study, we introduce an automatic unilateral ICA segmentation that is sensitive to steno-occlusive ICA. Moreover, we aim to extend the modified IDIF method into specific clinical trial to preliminary evaluate the potential of CMRGlc and further to monitor the pathophysiological changes.

Materials And Methods

The experimental framework was presented in Fig.1. This study was composed of three steps: A) Image process pipeline, which introduced the two quantitative approach, modified IDIF and SUVR process, B) IDIF validation, which introduced the CMRGlc's validity in healthy controls, C) IDIF application, which introduced the diagnostic assessment and postoperative measurement in ischemic cerebrovascular disease patients.

Participants

The data were collected during a hybrid TOF PET/MR system (Signa, GE Healthcare) imaging study conducted from June 2017 through January 2021 in the Department of Radiology and Nuclear Medicine at Xuanwu Hospital Capital Medical University, which included 26 ischemic cerebrovascular disease patients (22 male and 4 female, 50.2±8.6 y) with preoperative and postoperative imaging examination. The detailed diagnosis-specific exclusion and inclusion criteria included: 1) patients were confirmed diagnosis of ICA or MCA occlusive disease based on digital subtraction angiography; 2) evidence of cerebral hypoperfusion on CT or MR perfusion imaging consistent with affected side; 3) patients had a history of transient ischemic attacks or complete stroke involving the relevant ICA or MCA territory and treatment with ineffective medication[18]; 4) all patients completed PET-MR imaging within 1 month before STA-MCA bypass surgery and had confirmed vascular connection success based on digital subtraction angiography after surgery.

Patients were excluded if 1) had an acute stroke (less than one month); 2) ICA or MCA occlusion presented bilaterally; 3) with any contraindication for MRI and artefacts on MRI [19]. The severity of cerebrovascular diseases was measured using the National Institutes of Health Stroke Scale (NIHSS) and the Modified Rankin Scale (mRS). An imaging control group included 16 healthy controls (HCs, 5 male and 11 female, 46.8±10.6 y) were recruited from the community. HCs were chosen based on negative screening for neurological disorders, structural MRI images and MR angiography (MRA) image [20].

This study has been approved by the institutional review board of Xuanwu Hospital and conducted in accordance with the Declaration of Helsinki, and written informed consent was obtained from all subjects prior to the examinations.

PET/MR acquisition protocol

PET and MR sequence images were simultaneously acquired as shown in Supplementary Fig.1. Dynamic PET and MR images of all subjects were acquired on a hybrid PET/MR system (Signa, GE Healthcare). Each subject was instructed to fast for at least 6 h to reach a serum glucose level lower than 8 mmol/L. Before scanning, each subject was measured the glucose concentration (mmol/L) in blood. All imaging sessions were acquired in the resting state, without performing any task. A 19-channel head and neck union coil were used so that undertake a high signal-to-noise ratio of the PET/MR imaging. All subjects were placed in a supine position to ensure in the center of the field of view, and instructed to remain calm with their eyes closed.

Multiple MRI sequences included: a T1-weigthed MRI sequence (voxel size, 1×1×1 mm; echo time (TE), 3.2 ms; repetition time (TR), 8.5 ms; matrix, 256×256; 178 slices) for the anatomic localization, MR angiography (MRA) sequence (voxel size, 0.43×0.43×0.7 mm; TE, 3.7 ms; TR, 25 ms; matrix, 512×512; 272 slices) for the segmentation of the internal carotid vasculature, and a T2 fluid-attenuated inversion recovery (FLAIR) sequence (voxel size, 0.47×0.47×4 mm; TE, 144 ms; TR, 11000 ms; matrix, 512×512; 32 slices) for the definition of infarction area. At the same time, PET list-model acquisition was initiated with manual intravenous injection of ^{18}F-FDG (3.7 MBq/kg) and a 70-min dynamic PET image was acquired.

After scanning, the PET list mode data were re-binned into a dynamic frame sequence with 31 frames (10s×9, 30s×3, 60s×4, 180s×6, 300s×9; voxel size, 1.17×1.17×2.78 mm; matrix, 256×256; 89 slices) [12, 17, 21]. Corrected PET data were reconstructed using a time-of-flight, point spread function, ordered subset expectation maximization (TOF+PSF+OSEM) with 8 iterations and 28 subsets, and a 3-mm cut-off filter. Meanwhile, a single static PET frame was also reconstructed (50-60 min, voxel size: 1.82×1.82×2.78 mm; matrix, 192×192; 89 slices). All PET emission data were corrected for attenuation, scatter, random, decay, and deadtime. Attenuation correction was performed based on MR images, and the default attenuation correction sequence (Dixon MR sequences) was automatically prescribed and acquired as follows: LAVA-Flex (GE Healthcare) axial acquisition, voxel size = 1.95×2.93×5.2 mm, TE, 1.7 ms, TR, 4 ms, and 120 slices. Corrected PET data were reconstructed using TOF+PSF+OSEM algorithm with 8 iterations and 32 subsets, and a 3-mm cut-off filter.

IDIF method

Dynamic FDG-PET scans were analyzed using a fully automated processing pipeline to obtain an IDIF and further support the noninvasive absolute quantification of CMRGlc as described previously [16, 17]. The processing pipeline was denoted in Fig.1A. Firstly, individual TOF-MRA image was used to segment ICA by the automated carotid arteries segment method [16]. The petrous segment of ICA was regarded as VOI to extract IDIF. Of note, the unilateral ICA mask was acquired for ischemic cerebrovascular disease patients because of their progressive ICA steno-occlusive changes. The whole carotid

vasculature (CV) was identified using histogram-based quantile thresholding (0.995) and automatic seeded region growing with a connectedness constraint. According to ICA's specific morphology, we employed morphological feature vector (Gz) to characterize the shape of the vascular tree, according to the mathematical equation:

$$Gz = Nz \times Mz \times Rz \quad (1)$$

where normalized mean intensity (*Nz*), major axis length (*Mz*) and ratio of major to minor axis length (*Rz*) were obtained for CV slices with each cerebral hemisphere. The feature curve with elliptical structures presented as prominent peaks. The structure with the global max peak was regarded as the petrous segment. For patients with steno-occlusive ICA, the corresponding Gz peak of infraction side would lower than other structures. Along the slices from caudal to cranial, the ICA with lower Gz peak compared with last peak (circle of Willis) was regarded as steno-occlusive ICA and further removed from ICA mask. The above steps resulted in unilateral ICA mask for ischemic cerebrovascular disease patients, but bilateral ICA mask for HCs.

The individual T1-MRI sequence was regarded as the reference volume and all subsequent MRI scans were rigidly co-registered to native space (SPM 12, Wellcome Trust Center for Neuroimaging, UCL). All dynamic PET images were corrected for motion by rigid co-registration between each frame with the individual T1-MRI image. Subsequently, a modified Mueller-Gaertner method with spill-out and spill-in corrections was employed for partial volume effect (PVE) correction [16, 22]. The IDIF was derived and interpolated with a step length of 1. The voxel-wise Patlak graphical analysis was employed to generate the absolute CMRGlc map by the time-activity curve (IDIF) derived from corrected PET frames [23, 24]. For the assessment of the potential of noninvasive quantification modeling, the SUVR map was obtained by count normalizing each voxel's intensity to the mean activity concentration in whole cerebellum (Supplementary methods).

The supratentorial cerebral arterial territories are of key clinical importance for evaluation of cerebrovascular diseases and may help in the assessment of actual territorial contribution of individual collateral arteries in ischemic cerebrovascular disease patients [25, 4]. We employed this vascular territory to compare the performance of two quantitative methods. Vascular territory mapping including left and right anterior, middle, and posterior cerebral artery (ACA, MCA, and PCA), basilar artery (BA), and cerebellar artery (CA) territory in the standard space (Supplementary Fig.2) were manually drawn by two radiologists according to the maps described previously [26, 27]. All territories were warped to individual native space using deformation parameters. The average ipsilateral (surgery side, and excluding the infraction region) metabolic values of VOIs (gray matter, white matter, and 5 territories) were extracted from CMRGlc and SUVR maps for further analysis. The infraction area of each patient was available from T2-FLAIR sequence by two experienced radiologists. Each radiologist independently reviewed the infarction areas on FLAIR images in blind model. The resulting infarction volume was available by taking the average of two individual reader infarction areas.

IDIF validation and application

Consider the steno-occlusive ICA for ischemic cerebrovascular disease patients, the IDIF method used only unilateral ICA mask as blood-pool region to extract IDIF curve. To ensure that the quantification results were not influenced by unilateral ICA, we hypothesized that the quantification results derived from bilateral ICA should be similar to those of unilateral ICA. To test it, we compared quantitative CMRGlc results of bilateral ICA with those of unilateral ICA by characterizing the within-subject concordance in healthy controls. We used the intraclass correlation coefficient (ICC) and absolute percentage error to measure consistency between unilateral and bilateral CMRGlc values. We quantified and compared the CMRGlc values within 7 VOIs from healthy controls subjects, respectively.

To assess whether the IDIF quantification could accurately track the pathophysiological changes and the postoperative recovery effect, we calculated and compared the quantitative values derived from CMRGlc and SUVR maps for ischemic cerebrovascular disease pre- and post- operative visits using univariate ANOVAs with post-hoc tests. We evaluated which quantitative value was sensitive to metabolic abnormality and pathophysiological changes in ischemic cerebrovascular disease progression. We applied metabolic values of vascular territories into diagnostic assessment to classify the healthy controls and pre- and post- operative ischemic cerebrovascular disease patients *via* receiver operating characteristic curve (ROC). The relative change index, (postoperative value / preoperative value-1)*100%, was employed to measure the metabolic changes after surgery. Furthermore, to illustrate which quantitative value could track the degree of ischemic cerebrovascular severity, we used the general linear model to evaluate the association between clinical assessments (NIHSS and mRs scores) and quantitative values of surgery side cerebral hemispheres.

Statistical analyses

All average data were reported as mean ± standard deviation. Before statistical test, all variances were statistically analyses using normality tests. Metabolic difference across subjects were assessed separately using pared *t*-test, 1-way ANOVA and post hoc Dunnett tests. ROC and area under the curve (AUC) were employed to assess the diagnostic ability of quantitative values, and DeLong test was sued to measure the diagnostic differences [28]. All statistical analyses were conducted using SPSS software, version 24 (IBM). All measurements were considered significant at the $P<0.05$ level, two-tailed.

Results

Demographic information of all subjects was summarized in Table 1. All patients underwent PET/MR imaging at the preoperative visit and the postoperative follow-up visit (mean time interval, 7.9 days). And 59% ($n = 16$) presented the right steno-occlusive ICA and underwent right STA-MCA bypass surgery, 89% ($n = 24$) with infraction (average size, 13679 mm^3, range, 168-47267mm^3). The cohorts did not differ on other clinical characteristics except the gender ($P = 0.005$).

Petrous ICA mask segmentation had successfully identified the bilateral mask in HCs and the unilateral mask in patients (Supplementary Fig.3). Time activity curves derived from raw and PVE-corrected IDIF indicated that PVE correction mainly increased the intensities at the early frames of the IDIF, and may recover the actual intensity signal in petrous ICA (Supplementary Fig.4). Fig.2 shows the sample quantitative maps of different analysis methods for representative patients. Comparisons between IDIF and semi-quantitative method demonstrated that CMRGlc values subjectively captured excellent quantitative changes between pre- and post- operative images.

For IDIF quantification in HCs, time activity curves derived from unilateral and bilateral ICA masks are shown in Fig.3A. There was no significant difference between the computed time activity curves obtained from unilateral (left/right) and bilateral in healthy control, which emphasized that both unilateral and bilateral ICA mask could track similar time–activity curves using IDIF method.

CMRGlc values derived from both unilateral and bilateral IDIF within healthy controls were presented in Table 2. There were no significant differences for region CMRGlc values across bilateral and unilateral ICA measurements (all $P > 0.05$, ANOVA with Dunnett tests). There was higher within-subject concordance, and ICC between unilateral and bilateral CMRGlc values across VOIs were 0.91-0.98 (left) for the left comparison and 0.93-0.98 for the right comparison. Meanwhile, the absolute percentage errors between CMRGlc values across VOIs were 2.8%-5.6% and 2.8%-6.2% for the left and right IDIF comparison, respectively. Furthermore, Bland-Altman plots shows that CMRGlc values within the GM and WM demonstrated greater consistency characterized by unilateral and bilateral IDIF methods (Fig.3B and Fig3.C). Similar findings were obtained for other cerebral arterial territories (Supplementary Fig.5).

Average CMRGlc values on the ipsilateral side (not including the infarction area) were displayed in Table 3. Significant differences in CMRGlc were observed across the cohorts in all territories ($F_{(2,65)}$: 23.2-45.1, P< 0.001). For HCs, ipsilateral CMRGlc was high for all territories compared to the patients' cohorts (P < 0.01, Dunnett tests). In patient group, increased ipsilateral CMRGlc after surgery was evident in all vascular territories (P < 0.01, Dunnett tests).

There was a significant differences in SUVR across the cohorts in 4 territories (exclusion ACA, $F_{(2,65)}$: 23.2-45.1, P< 0.01). Changed SUVRs between pre- and post-operative visits were significantly observed only in the PCA and CA territories (P < 0.05, Dunnett tests). Based on the patient's results, the CMRGlc values were significantly increased after surgery treatment (P < 0.05) for all territories (range: 7.4%~22.5%, Fig.4A). However, the corresponding SUVR values only in the PCA and BA regions (-2.8% and 1.9%) were significant different (P < 0.05, Fig.4B).

The diagnostic results of quantitative values were shown as Fig.5. For 2-class classification (HC and ischemic cerebrovascular disease), the diagnostic ability of CMRGlc in vary territories (AUC: 0.923-0.966) were significantly higher than of SUVR (AUC: 0.697-0.826) (P < 0.05, DeLong test; Supplementary Table 1). Comparison results indicates CMRGlc values sensitively captured the glucose metabolism changes in vascular territories.

There was a significant association between CMRGlc values with NIHSS scores (r: -0.54, P = 0.0041), in contrast with weaker correlations with SUVR and NIHSS (r: -0.18, P = 0.37, Fig.6). However, there was no significant association between mRS and quantitative values (CMRGlc: r: -0.14, P = 0.48; SUVR: r: -0.03, P = 0.89; Supplementary Fig.6). The above results indicated that CMRGlc could effectively track the degree of ischemic cerebrovascular severity.

Discussion

This study highlighted the characterization of pathophysiological changes and vascular territory metabolism in ischemic cerebrovascular disease patients with unilateral steno-occlusive ICA based on noninvasive quantification of CMRGlc and dynamic FDG imaging with hybrid PET/MR system. We attempted to propose the quantification approach of ischemic cerebrovascular disease that advances the PET application in the cerebrovascular disease. Indeed, the results showed that the noninvasive IDIF based on unilateral ICA maybe a potential approach for clinical PET quantification and provide greater absolute measures of vascular metabolism.

Ischemic cerebrovascular disease is the most common cause of death and the major cause of disability worldwide. PET quantitative analysis is the main parameter of brain function after stroke. Recapitulating previous studies about cerebrovascular disease, these works had focused on the regional hemodynamic and metabolic changes by radionuclide imaging [29, 3, 30, 12]. However, PET quantification still suffered from specific ischemic cores, unilateral steno-occlusive ICA, and insufficient sensitivity for the cerebrovascular disease. One means to address these potential pitfalls was through absolute quantification. Due to arterial blood sampling is invasive, researchers present clinically viable approach to extract an IDIF for the determination of CMRGlc using integrated PET/MR [31]. Sundar *et al* calculated CMRGlc based on the standard rate constant approach and this study was performed with healthy volunteers [16]. Su *et al* validated an IDIF technique and observed asymmetry in the ischemic cerebrovascular disease patients [5]. But as discussed in previous works, these studies used bilateral ICA to measure CMRGlc and it maybe not suitable for unilateral ICA steno-occlusive disease. In our study, we developed an adaptive segmentation algorithm to define the contralateral ICA region of ischemic cerebrovascular disease patients. We first used both unilateral and bilateral ICA approach to extract an IDIF for PET quantification in HCs. We compared the CMRGlc quantification performance, and the result showed IDIF based unilateral and bilateral ICA regions generated similar CMRGlc values within each VOI (absolute percentage errors range: 2.8%-6.2%). There was no significant difference between these ICA measurements. The validation in HCs indicated that using only unilateral ICA as a region to extract IDIF could track accurate glucose metabolism activity. Our results indicated that the CMRGlc values of GM (34.9±6.3 umol/100g/min) were consistent with the previous results (32±6 umol/100g/min) based on IDIF method [16]. Many studies reported that the normal adults have an average whole brain

CMRGlc approximately of 25-35 μmol/100 g/min [32, 33]. Our results also show that the average CMRGlc is 24.54 μmol/100 g/min. It suggested that this method had successfully applied into our central data. Considering that the predominance of simultaneous PET/MR data acquisition and the feasibility of IDIF approach, the noninvasive quantification may be useful to cerebrovascular applications.

In our study, we focused on the IDIF approach into the ischemic cerebrovascular disease patients to evaluate whether detailed changes that occurred in glucose metabolism between before and after bypass surgery. Converging studies suggested that bypass surgery contribute to increase blood flow to the affected hemisphere and reduce the risk of ensuing neuronal damage in patients. Yu Z *et al*. previously reported the glucose metabolism values were increased after surgery [10]. However, little research has focused on the change of CMRGlc values in chronic stroke. Nagasawa H et al found that there were significantly decreased CMRGlc on affected side which compared control subjects using ^{18}F-FDG PET in 7 patients with chronic ischemic cerebrovascular disease [34]. Our results showed that the CMRGlc values of patients in vascular territories were lower than HCs, and the postoperative values were significant increased than preoperative values. The increased CMRGlc may indicate that surgery contribute to prevent irreversible ischemic damage and recover part glucose feeding in steno-occlusive artery disease. Kao et al reported successful surgery treatment may improve long-term cerebral glucose metabolism in patients with chronic severe carotid stenosis or occlusion [9]. However, in our study, the metabolism recovery in various territory (7.4%~22.5%) narrowed the gap of healthy but still significant increase. It may be caused by short follow-up period and the promotion of glucose metabolism seems to involve a slower process.

Further, experimental results indicated the feasibility of quantification of CMRGlc in the ischemic cerebrovascular disease trial using hybrid PET/MR, without the need for reference regions or invasive arterial blood sampling. Our previous study suggested that there was no significant increase in SUVR between pre- and post-operative measurements, while the asymmetry index of SUVR had significant changed [12]. In the present study, the comparison results demonstrated CMRGlc had better performance than SUVR in tracking pathophysiological changes (Supplemental Table 1). For the quantitative results, CMRGlc captured more sensitive and complete metabolic changes, especially in the recovery effect after surgery. SUVR values were failed to track the metabolism changes and even obvious abnormality in PCA territory. Previous study showed that SUV value in the ischemic hemisphere could be sensitive sensitive indicator for predicting ischemia, but not only the ipsilateral SUV value but also the contralateral SUV value showed changes after surgery treatment in 1 month [35]. Moreover, the application of SUVR may be blind to the metabolism changes in the ipsilateral cerebellum region (BA territory) because of the reference region. Furthermore, we also measured the significant relationship between quantitative values and clinical stroke assessment (NIHSS) in preoperative ischemic cerebrovascular disease patients, in line with a previous study [36]. CMRGlc can serve as a potential surrogate of the severity of the damage.

There are several limitations for improvement. First, we did not obtain the arterial blood sampling as the reference standard to further evaluate the application of IDIF in cerebrovascular disease. Secondly, the small sample size with heterogeneity and lack of randomization limited the interpretation of our data. Future studies with larger patient numbers (including patients with and without bypass surgery) and longer follow-up periods are warranted.

In conclusion, this study proposes an ischemic cerebrovascular disease quantification protocol based on automated noninvasive processing and dynamic FDG imaging with hybrid TOF PET/MR system, not previously applied to the cerebrovascular disease. This approach sheds new light on the quantification of CMRGlc for ischemic cerebrovascular disease patients and advances the mechanism understanding for the alterative recovery strategies and permit the personalized precision intervention.

Declarations

Funding

This work was supported by grants from the National Natural Science Foundation of China (Grant No. 81974261 and 82020108013), Beijing Natural Science Foundation (Z190014), Beijing Municipal Administration of Hospitals' Ascent Plan (No. DFL20180802), Shanghai Municipal Science and Technology Major Project (No. 2017SHZDZX01, 2018SHZDZX03), the 111 Project (No. D20031). No other potential conflicts of interest relevant to this article exist.

Competing interests

The authors report no competing interests.

Availability of data and material

The data that support the findings of this study are available from the corresponding author, upon reasonable request.

Research involving human participants and/or animals

The research involved human participants. This retrospective study was permitted by the Research Ethics Committee of the Capital Medical University of Xuanwu hospital.

Consent to participate

All patients gave written informed consent prior to enrollment in this study.

References

1. Evans NR, Tarkin JM, Buscombe JR, Markus HS, Rudd JHF, Warburton EA. PET imaging of the neurovascular interface in cerebrovascular disease. Nat Rev Neurol. 2017;13(11):676-88. doi:10.1038/nrneurol.2017.129.
2. van Laar PJ, van der Grond J, Hendrikse J. Brain perfusion territory imaging: methods and clinical applications of selective arterial spin-labeling MR imaging. Radiology. 2008;246(2):354-64. doi:10.1148/radiol.2462061775.
3. Heiss WD. PET imaging in ischemic cerebrovascular disease: current status and future directions. Neurosci Bull. 2014;30(5):713-32. doi:10.1007/s12264-014-1463-y.
4. Heidari Pahlavian S, Geri O, Russin J, Ma SJ, Amar A, Wang DJJ et al. Semiautomatic cerebrovascular territory mapping based on dynamic ASL MR angiography without vessel-encoded labeling. Magn Reson Med. 2021;85(5):2735-46. doi:10.1002/mrm.28623.
5. Su Y, Vlassenko AG, Couture LE, Benzinger TL, Snyder AZ, Derdeyn CP et al. Quantitative hemodynamic PET imaging using image-derived arterial input function and a PET/MR hybrid scanner. J Cereb Blood Flow Metab. 2017;37(4):1435-46. doi:10.1177/0271678x16656200.
6. Wang J, Chao F, Han F, Zhang G, Xi Q, Li J et al. PET demonstrates functional recovery after transplantation of induced pluripotent stem cells in a rat model of cerebral ischemic injury. J Nucl Med. 2013;54(5):785-92. doi:10.2967/jnumed.112.111112.
7. Bunevicius A, Yuan H, Lin W. The potential roles of 18F-FDG-PET in management of acute stroke patients. Biomed Res Int. 2013;2013:634598. doi:10.1155/2013/634598.

8. Pyatigorskaya N, Habert MO, Rozenblum L. Contribution of PET-MRI in brain diseases in clinical practice. Current opinion in neurology. 2020;33(4):430-8. doi:10.1097/wco.0000000000000841.
9. Hsien-Li K, Mao-Shin L, Wen-Chau W, Tseng WYI, Mao-Yuan S, Ya-Fang C et al. Improvement of Cerebral Glucose Metabolism in Symptomatic Patients With Carotid Artery Stenosis After Stenting. Clinical Nuclear Medicine. 2015;40(9):701-7.
10. Yu Z, Shi X, Qian H, Liu F, Zhou Z, Sun Y et al. Internal maxillary artery to intracranial artery bypass: a case series of 31 patients with chronic internal carotid/middle cerebral arterial-sclerotic steno-occlusive disease. Neurological research. 2016;38(5):420-8. doi:10.1080/01616412.2016.1177931.
11. Heiss WD. Hybrid PET/MR Imaging in Neurology: Present Applications and Prospects for the Future. J Nucl Med. 2016;57(7):993-5. doi:10.2967/jnumed.116.175208.
12. Cui B, Zhang T, Ma Y, Chen Z, Ma J, Ma L et al. Simultaneous PET-MRI imaging of cerebral blood flow and glucose metabolism in the symptomatic unilateral internal carotid artery/middle cerebral artery steno-occlusive disease. Eur J Nucl Med Mol Imaging. 2020;47(7):1668-77. doi:10.1007/s00259-019-04551-w.
13. Lanz B, Poitry-Yamate C, Gruetter R. Image-derived input function from the vena cava for 18F-FDG PET studies in rats and mice. J Nucl Med. 2014;55(8):1380-8. doi:10.2967/jnumed.113.127381.
14. Sommer WH, Bollwein C, Thierfelder KM, Baumann A, Janssen H, Ertl-Wagner B et al. Crossed cerebellar diaschisis in patients with acute middle cerebral artery infarction: Occurrence and perfusion characteristics. J Cereb Blood Flow Metab. 2016;36(4):743-54. doi:10.1177/0271678x15617953.
15. Khalighi MM, Deller TW, Fan AP, Gulaka PK, Shen B, Singh P et al. Image-derived input function estimation on a TOF-enabled PET/MR for cerebral blood flow mapping. J Cereb Blood Flow Metab. 2018;38(1):126-35. doi:10.1177/0271678x17691784.
16. Sundar LK, Muzik O, Rischka L, Hahn A, Rausch I, Lanzenberger R et al. Towards quantitative [18F]FDG-PET/MRI of the brain: Automated MR-driven calculation of an image-derived input function for the non-invasive determination of cerebral glucose metabolic rates. J Cereb Blood Flow Metab. 2019;39(8):1516-30. doi:10.1177/0271678X18776820.
17. Shiyam Sundar LK, Muzik O, Rischka L, Hahn A, Lanzenberger R, Hienert M et al. Promise of Fully Integrated PET/MRI: Noninvasive Clinical Quantification of Cerebral Glucose Metabolism. J Nucl Med. 2020;61(2):276-84. doi:10.2967/jnumed.119.229567.
18. Powers WJ, Clarke WR, Grubb RL, Jr., Videen TO, Adams HP, Jr., Derdeyn CP. Extracranial-intracranial bypass surgery for stroke prevention in hemodynamic cerebral ischemia: the Carotid Occlusion Surgery Study randomized trial. Jama. 2011;306(18):1983-92. doi:10.1001/jama.2011.1610.
19. Miyamoto S, Yoshimoto T, Hashimoto N, Okada Y, Tsuji I, Tominaga T et al. Effects of extracranial-intracranial bypass for patients with hemorrhagic moyamoya disease: results of the Japan Adult Moyamoya Trial. Stroke. 2014;45(5):1415-21. doi:10.1161/strokeaha.113.004386.
20. Cha YH, Jog MA, Kim YC, Chakrapani S, Kraman SM, Wang DJ. Regional correlation between resting state FDG PET and pCASL perfusion MRI. J Cereb Blood Flow Metab. 2013;33(12):1909-14. doi:10.1038/jcbfm.2013.147.
21. Zhou Y, Ye W, Brasić JR, Crabb AH, Hilton J, Wong DF. A consistent and efficient graphical analysis method to improve the quantification of reversible tracer binding in radioligand receptor dynamic PET studies. Neuroimage. 2009;44(3):661-70. doi:10.1016/j.neuroimage.2008.09.021.
22. Müller-Gärtner HW, Links JM, Prince JL, Bryan RN, McVeigh E, Leal JP et al. Measurement of radiotracer concentration in brain gray matter using positron emission tomography: MRI-based correction for partial volume effects. J Cereb Blood Flow Metab. 1992;12(4):571-83. doi:10.1038/jcbfm.1992.81.
23. Patlak CS, Blasberg RG. Graphical evaluation of blood-to-brain transfer constants from multiple-time uptake data. Generalizations. J Cereb Blood Flow Metab. 1985;5(4):584-90. doi:10.1038/jcbfm.1985.87.

24. Graham MM, Muzi M, Spence AM, O'Sullivan F, Lewellen TK, Link JM et al. The FDG lumped constant in normal human brain. J Nucl Med. 2002;43(9):1157-66.
25. Momjian-Mayor I, Baron JC. The pathophysiology of watershed infarction in internal carotid artery disease: review of cerebral perfusion studies. Stroke. 2005;36(3):567-77. doi:10.1161/01.STR.0000155727.82242.e1.
26. Kim DE, Park JH, Schellingerhout D, Ryu WS, Lee SK, Jang MU et al. Mapping the Supratentorial Cerebral Arterial Territories Using 1160 Large Artery Infarcts. JAMA Neurol. 2019;76(1):72-80. doi:10.1001/jamaneurol.2018.2808.
27. Nowinski WL, Qian G, Kirgaval Nagaraja BP, Thirunavuukarasuu A, Hu Q, Ivanov N et al. Analysis of ischemic stroke MR images by means of brain atlases of anatomy and blood supply territories. Acad Radiol. 2006;13(8):1025-34. doi:10.1016/j.acra.2006.05.009.
28. DeLong ER, DeLong DM, Clarke-Pearson DL. Comparing the areas under two or more correlated receiver operating characteristic curves: a nonparametric approach. Biometrics. 1988;44(3):837-45.
29. Heiss WD. Radionuclide imaging in ischemic stroke. J Nucl Med. 2014;55(11):1831-41. doi:10.2967/jnumed.114.145003.
30. Heiss WD, Zaro Weber O. Validation of MRI Determination of the Penumbra by PET Measurements in Ischemic Stroke. J Nucl Med. 2017;58(2):187-93. doi:10.2967/jnumed.116.185975.
31. Huang Q, Massey JC, Minczuk K, Li J, Kundu BK. Non-invasive determination of blood input function to compute rate of myocardial glucose uptake from dynamic FDG PET images of rat heart in vivo: comparative study between the inferior vena cava and the left ventricular blood pool with spill over and partial volume corrections. Phys Med Biol. 2019;64(16):165010. doi:10.1088/1361-6560/ab3238.
32. Powers WJ, Zazulia AR. PET in Cerebrovascular Disease. PET Clinics. 2010;5(1):83-106. doi:10.1016/j.cpet.2009.12.007.
33. Villien M, Wey HY, Mandeville JB, Catana C, Polimeni JR, Sander CY et al. Dynamic functional imaging of brain glucose utilization using fPET-FDG. Neuroimage. 2014;100:192-9. doi:10.1016/j.neuroimage.2014.06.025.
34. Nagasawa H, Kogure K, Itoh M, Ido T. Multi-focal metabolic disturbances in human brain after cerebral infarction studied with 18FDG and positron emission tomography. Neuroreport. 1994;5(8):961-4. doi:10.1097/00001756-199404000-00027.
35. Yu Z, Shi X, Zhou Z, Yang Y, Li P, Zhang Y. Cerebral glucose metabolism changes in chronic ischemia patients following subcranial-intracranial bypass. Neurosurg Rev. 2019. doi:10.1007/s10143-019-01177-2.
36. Szilágyi G, Vas A, Kerényi L, Nagy Z, Csiba L, Gulyás B. Correlation between crossed cerebellar diaschisis and clinical neurological scales. Acta neurologica Scandinavica. 2012;125(6):373-81. doi:10.1111/j.1600-0404.2011.01576.x.

Tables

Table 1 Cohort Characteristics of all participants.

Characteristic	Healthy controls (n = 16)	Ischemic cerebrovascular disease patients (n = 26)		*P* value
		Preoperative	Postoperative	
Gender (M/F)	5/11	22/4		0.005[a]
Age (year)	46.8±10.6 (29-61)	50.2±8.6 (32-63)		0.262[b]
Follow-up (day)	\	7.9±2.0 (3-13)		\
NIHSS	\	1 (0-4)	\	\
mRS	\	1 (0-2)	\	\
Blood glucose (mmol/L)	5.74±0.55 (4.6-6.6)	5.78±0.72 (4.7-7.9)	5.87±0.72 (4.8-7.4)	0.78[c]
Injection (MBq)	268±44 (185-351)	286±45 (218-406)	283±48 (187-388)	0.84[c]

[a]Chi squared test.

[b]The two sample t test.

[c]The one-way analysis of variance (ANOVA).

Group count data or mean ± standard deviation (range) is shown. NIHSS and mRS is shown as median value (range). NIHSS: National Institutes of Health Stroke Scale. mRS: Modified Rankin Scale.

Table 2 Regional CMRGlc values in healthy controls (n = 16).

Region	Bilateral ICA	Unilateral ICA		ICC		Absolute percentage error	
		Left ICA	Right ICA	Left	Right	Left	Right
GM	34.9±6.3	34.7±6.4	35.5±6.9	0.97 (0.94-0.99)	0.98 (0.94-0.99)	3.1±2.3	2.8±2.1
WM	19.1±4.1	18.9±4.6	19.3±4.2	0.96 (0.89-0.98)	0.97 (0.91-0.99)	4.4±6.3	3.8±3.2
MCA	26.1±5.2	26.1±5.3	26.7±5.7	0.96 (0.89-0.98)	0.97 (0.91-0.99)	2.9±2.5	3.3±2.7
PCA	28.7±5.6	28.4±6.3	29.4±6.2	0.95 (0.88-0.98)	0.97 (0.91-0.99)	4.3±6.1	3.4±2.5
ACA	28.9±5.9	28.8±6.0	29.5±6.5	0.98 (0.95-0.99)	0.98 (0.93-0.99)	2.8±2.3	3.2±2.5
BA	17.8±4.8	17.7±4.7	18.3±4.0	0.95 (0.90-0.98)	0.93 (0.81-0.97)	5.5±6.7	5.4±5.9
CA	21.2±5.2	21.8±5.3	22.3±4.6	0.91 (0.81-0.96)	0.94 (0.80-0.98)	5.6±6.5	6.2±7.7

CMRGlc values were reported as μmol/100 g/min. Real value (95% confidence interval) or mean ± standard deviation is shown for ICC and absolute percentage error, respectively.

CMRGlc: cerebral metabolic rate for glucose. ICA: internal carotid artery. ICC: intraclass correlation coefficient. GM: grey matter. WM: white matter. MCA: middle cerebral artery. PCA: posterior cerebral artery. ACA: posterior cerebral artery. BA: basilar artery. CA: cerebellar artery.

Table 3 Ipsilateral metabolic measurements of subjects

Region	Cerebral metabolic rate for glucose				Standardized uptake value ratio			
	HCs	Preoperative	Postoperative	$F_{(2,65)}$	HCs	Preoperative	Postoperative	$F_{(2,65)}$
MCA	26.4±5.4	14.6±4.4	17.2±4.0	35.4**	1.08±0.07	0.98±0.08	1.00±0.08	8.3**
PCA	28.9±5.6	16.7±4.0	18.1±3.5	45.1**	1.14±0.07	1.08±0.08	1.05±0.07	8.1**
ACA	29.2±5.9	17.6±4.3	19.3±4.2	32.5**	1.14±0.08	1.08±0.09	1.08±0.09	2.6
BA	18.4±3.9	10.4±2.5	12.0±2.4	40.3**	0.79±0.03	0.76±0.03	0.77±0.04	6.2*
CA	21.9±4.7	14.1±3.2	16.5±3.2	23.2**	1.00±0.01	1.04±0.04	1.04±0.03	6.1*

P values were derived using paired t-test. Cerebral metabolic rate for glucose values were reported as umol/100 g/min.

* represents P < 0.01 and ** represents P < 0.001.

HCs: healthy controls. MCA: middle cerebral artery. PCA: posterior cerebral artery. ACA: posterior cerebral artery. BA: basilar artery. CA: cerebellar artery.

Figures

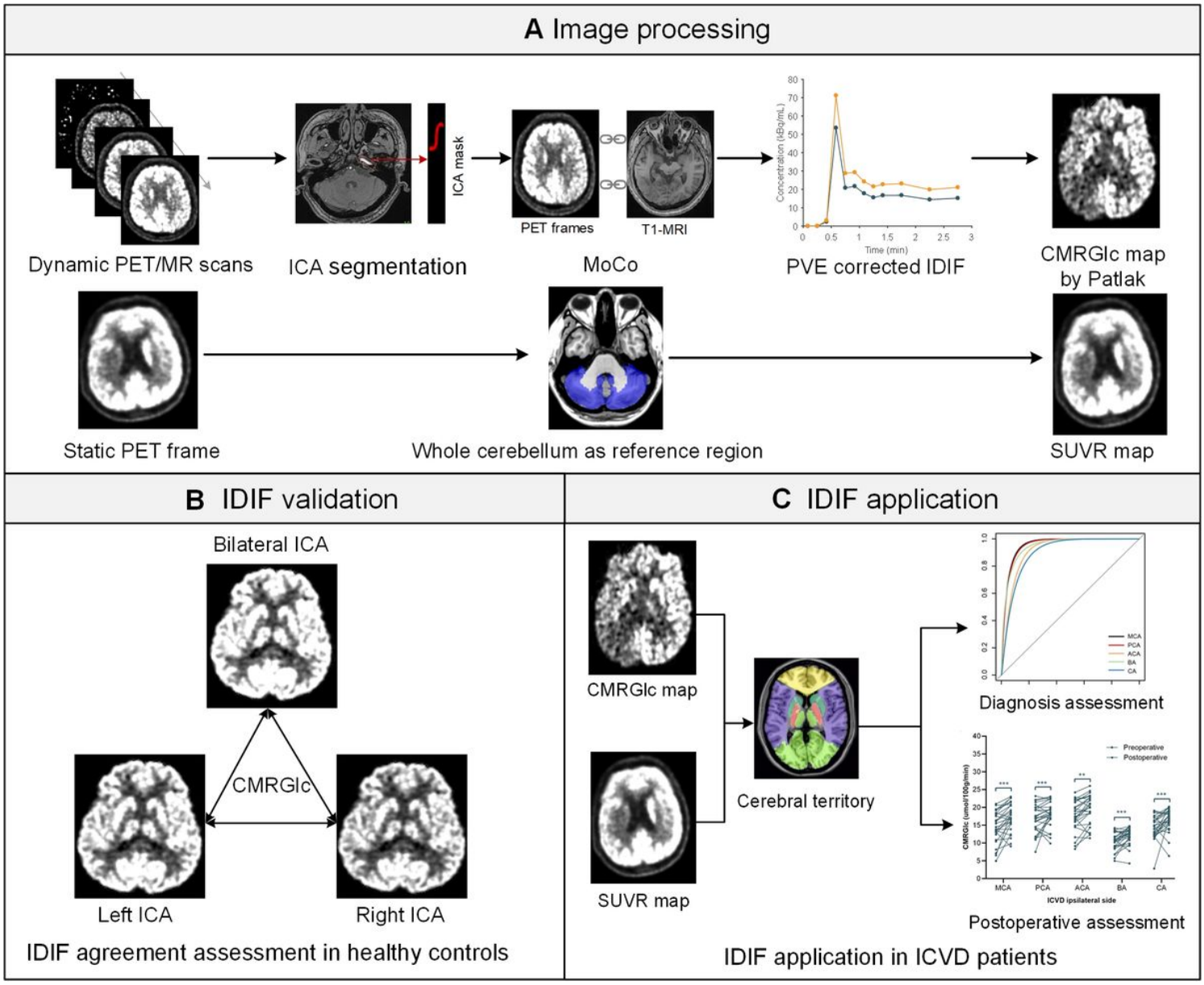

Figure 1

Experimental flowchart. The flowchart of image process pipeline (A), the IDIF validation in healthy controls (B), and the IDIF application and quantitative analyses (C).

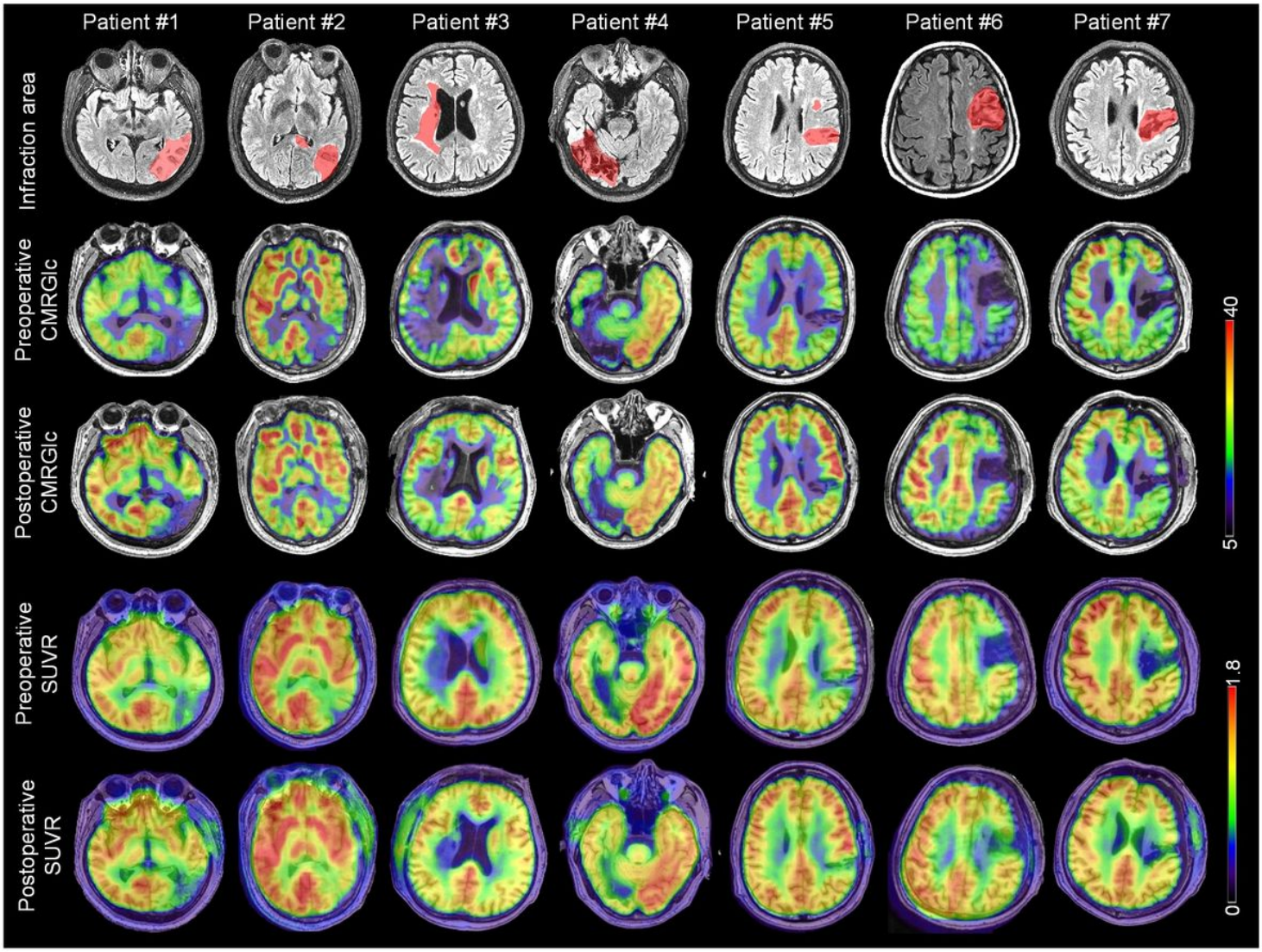

Figure 2

The CMRGlc and SUVR maps of 7 representative patients. Infarction area was acquired at preoperative visit and overlayed on the T2-FLAIR image. CMRGlc and SUVR maps were overlayed on the corresponding T1-MRI image.

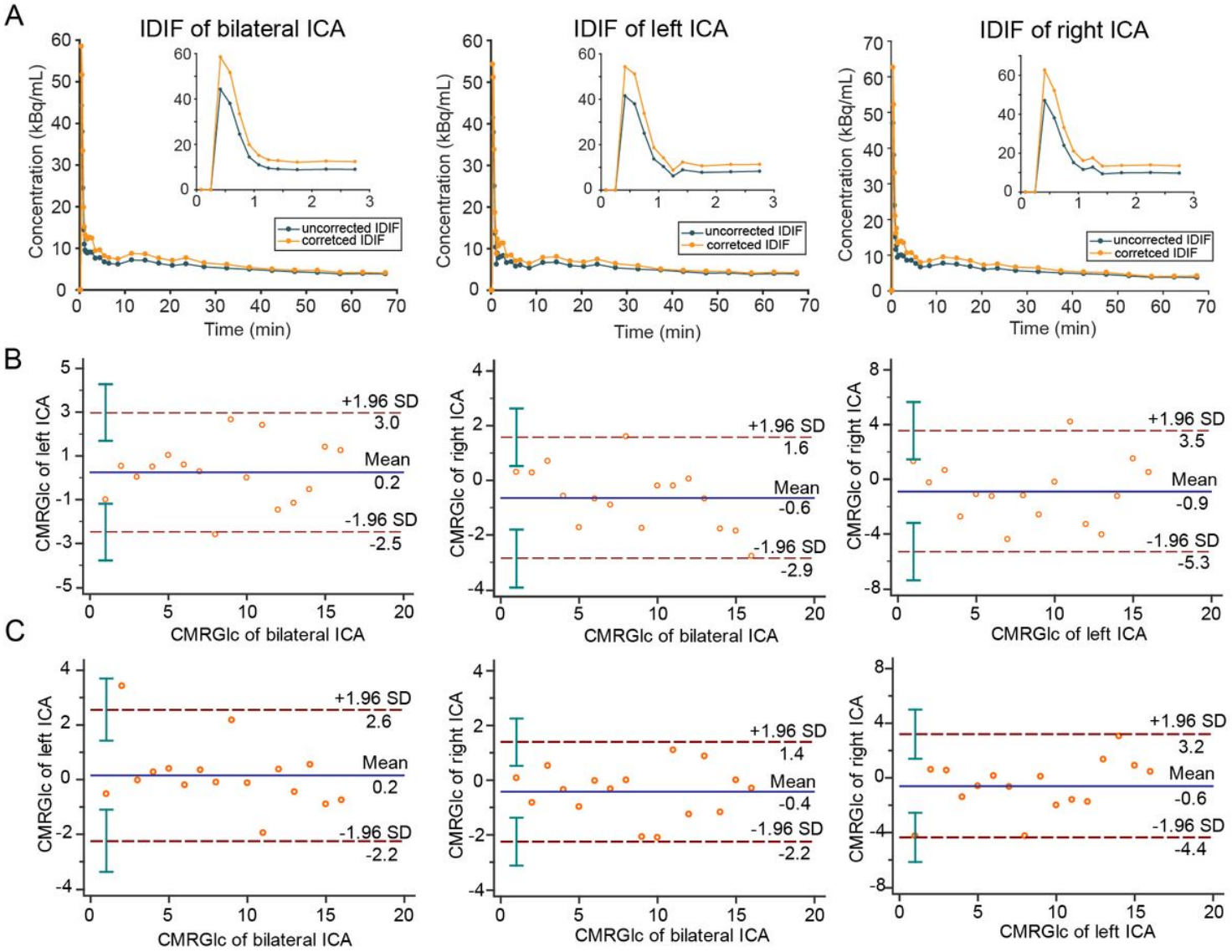

Figure 3

The quantification performance of unilateral and bilateral IDIF methods. (A) Time activity curves derived from bilateral, left, and right ICA obtained from a representative healthy control (Female, 42y). Bland-Altman plot of grey matter (B) and white matter (C) demonstrates close agreement for CMRGlc values from unilateral and bilateral IDIF.

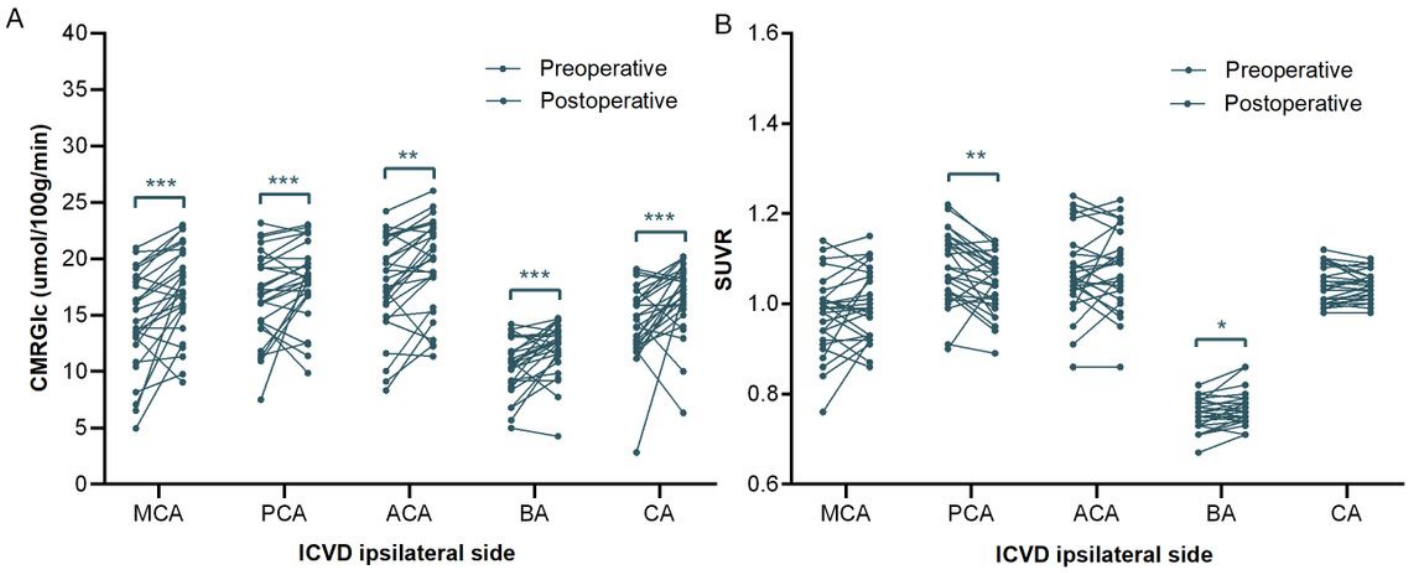

Figure 4

CMRGlc (A) and SUVR (B) values of ICVD patients at ipsilateral side. Dots represent individual quantitative values in pre- and post- operative visits. Asterisk represents different statistical powers (**, 0.01; ***, <0.001).

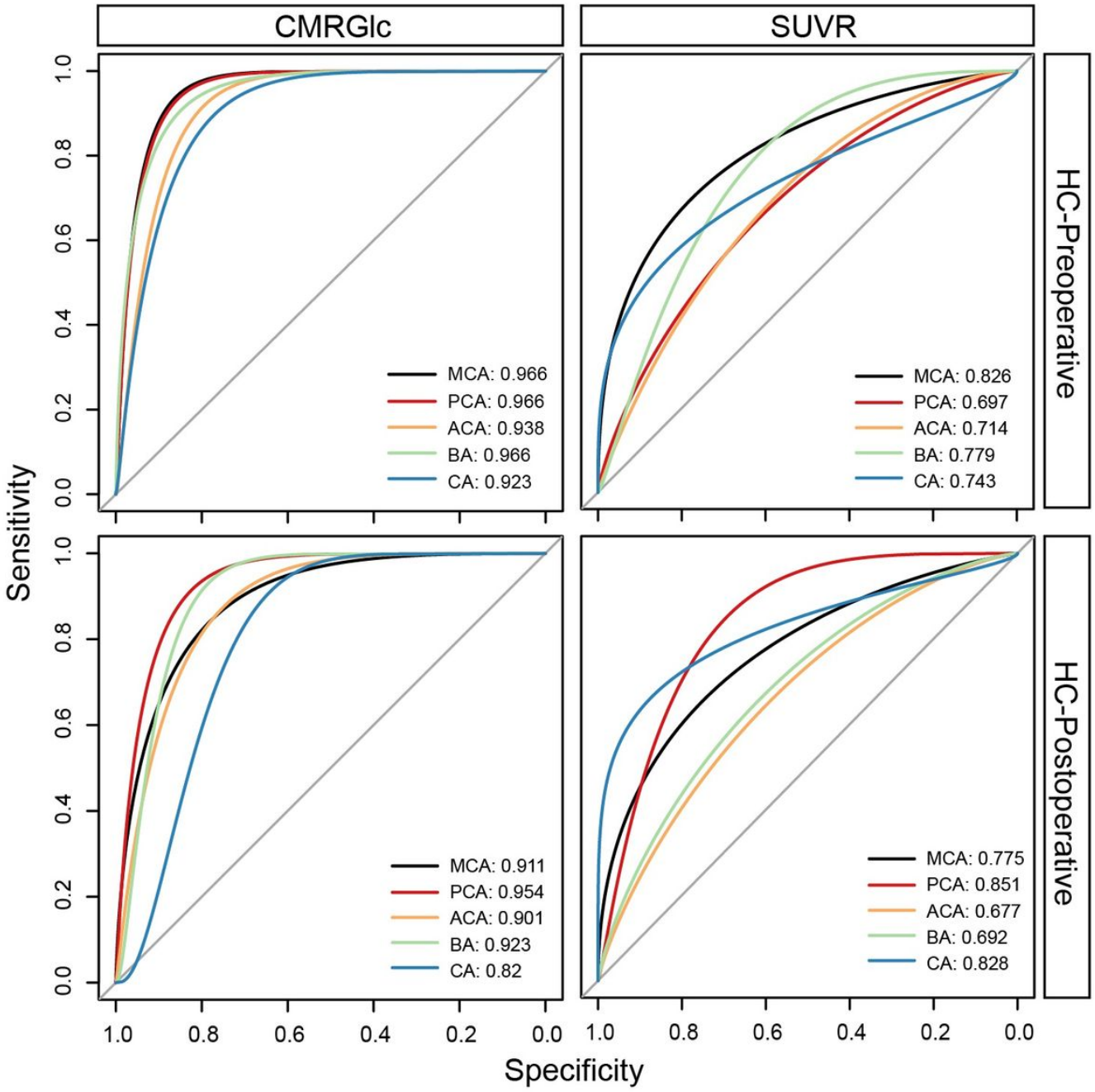

Figure 5

The ROC curves of the quantitative values in the healthy control (HC) and patients' groups. Different ROC' colors represent quantitative values of different vascular territories.

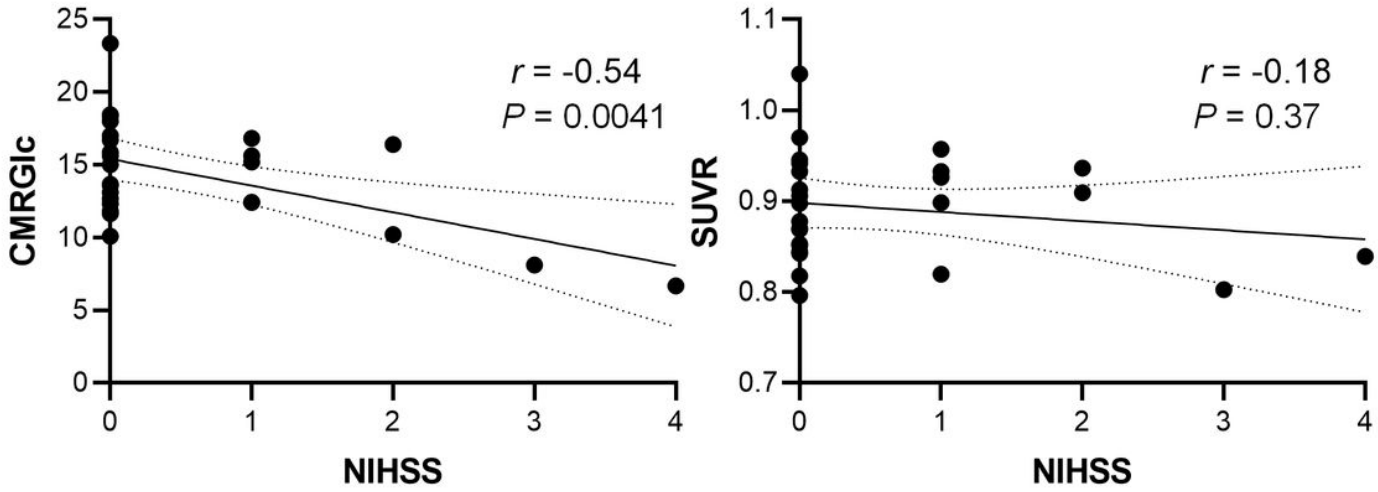

Figure 6

The relationship between NIHSS score and CMRGlc values (r = -0.54, left) and SUVR (r = -0.18, right).

Supplementary Files

This is a list of supplementary files associated with this preprint. Click to download.

- SupplementalMaterial.docx